(4) Šolc, K. *J. Chem. Phys.* **1971**, *55*, 335.
(5) Šolc, K.; Gobush, W. *Macromolecules* **1974**, *7*, 814.
(6) Stockmayer, W. H. *XXIVth International Congress of Pure and Applied Chemistry*; Butterworths: London, 1974; Vol. 1, p 91, and references therein.
(7) Eichinger, B. E. *Macromolecules* **1977**, *10*, 671.
(8) Eichinger, B. E. *Macromolecules* **1985**, *18*, 211.
(9) Muirhead, R. J. *Aspects of Multivariate Statistical Theory*; Wiley: New York, 1982; Chapter 7.
(10) Shy, L. Y.; Eichinger, B. E. *Macromolecules* **1986**, *19*, 838.
(11) Theodorou, D. N.; Suter, U. W. *Macromolecules* **1985**, *18*, 1206.
(12) Bishop, M.; Saltiel, C. J. *J. Chem. Phys.* **1986**, *85*, 6728.
(13) Aronovitz, J. A.; Nelson, D. R. *J. Phys. (Les Ulis, Fr.)* **1986**, *47*, 1445.
(14) Rudnick, J.; Gaspari, G. *Science* **1987**, *237*, 384.
(15) Rudnick, J.; Beldjenna, A.; Gaspari, G. *J. Phys. A: Math. Gen.* **1987**, *20*, 971.
(16) Gaspari, G.; Rudnick, J.; Beldjenna, A. *J. Phys. A: Math. Gen.* **1987**, *20*, 3393.
(17) Bishop, M.; Saltiel, C. J. *J. Chem. Phys.* **1988**, *88*, 3976.
(18) Abramowitz, M.; Stegun, I. A. *Handbook of Mathematical Functions*; National Bureau of Standards: Bethesda, 1970; *Applied Math. Sec. 55*, p 230.
(19) Coriell, S. R.; Jackson, J. L. *J. Math. Phys.* **1967**, *8*, 1276.
(20) *The IMSL Library, Reference Manual*, 9th ed.; International Mathematical and Statistical Libraries: Houston, TX, 1982; Programs MMDEI and MMBSIO.
(21) Gerald, C. F. *Applied Numerical Analysis*, 3rd ed.; Addison Wesley: Reading, MA, 1984; Chapter 4.
(22) Gradshteyn, I. S.; Ryzhik, I. M. *Table of Integrals, Series, and Products*; Academic Press: New York, 1965: Entry 8.212.6, p 925; Entry 9.261.1, p 1067.
(23) Press, W. H.; Flannery, B. P.; Teukolsky, S. A.; Vetterling, W. T. *Numerical Recipes*; Cambridge University Press: Cambridge, New York, 1986; Chapter 4.

Interpretation of Long-Chain Structure in Flexible Homopolymers from Dilute-Solution Dynamic Properties Measured in Good Solvents

Robert L. Sammler† and John L. Schrag*

Department of Chemistry and Rheology Research Center, University of Wisconsin, Madison, Wisconsin 53706. *Received September 16, 1988; Revised Manuscript Received January 27, 1989*

ABSTRACT: Non-Gaussian effects on the frequency dependence of intrinsic birefringence or intrinsic viscoelasticity are investigated for flexible homopolymers in dilute solution. The effects are examined for bead–spring model chains having linear or regular star geometry by using the approximate framework of Ptitsyn and Eizner. Predicted properties are computed for chains of finite size for both uniform and nonuniform chain expansions; the results are compared to those of the Gaussian model. These comparisons clarify why measured dynamic properties of flexible homopolymers dissolved in good solvents often correspond quantitatively to properties computed for the Gaussian model. Long-chain structure parameters obtained by fitting measured dynamic properties with Gaussian model predictions are expected to be at most weakly dependent on solvent power.

I. Introduction

The frequency dependence of the modified intrinsic birefringence $[S^*]_\Delta$ and viscoelasticity $[\eta^*]_\Delta$ has recently[1] been shown to have excellent potential for characterization of long-chain structure in monodisperse samples of flexible homopolymers. However, these low-shear-rate predictions were based on a Gaussian chain model that makes them most applicable to measured properties of homopolymers in Θ solvents. Properties in Θ solvents—especially required to characterize long-chain structure—are particularly difficult to obtain relative to those in good solvents; the signals are lower and the accessible effective frequency range is much smaller since time–temperature superposition techniques[2] are no longer applicable. Properties in Θ solvents are also less sensitive to long-chain structure because the breadth of the relaxation time spectrum characterizing the conformational motions of a chain in solution compresses as the solvent power diminishes. These concerns make the measurement of solution properties in good solvents much more attractive, though the interpretation of long-chain structure from such properties is complicated by the lack of a rigorous, mathematically tractable theory quantitatively predicting these properties for non-Gaussian chains. Fortunately, as summarized in ref 1, the Gaussian model has been surprisingly successful in fitting properties measured in good solvents; this has been done by experimentalists for at least 20 years.[2] Strictly speaking, the interpretation of the fit parameters has not been entirely clear because of the non-Gaussian nature of the real chains; our purpose here is to investigate non-Gaussian effects on the fit parameters. Non-Gaussian effects are predicted with the bead–spring model formulated in the approximate framework of Ptitsyn and Eizner;[3-5] chains of finite size and various degrees of hydrodynamic interaction are considered. These predictions are then fit by those of the Gaussian bead–spring model. Differences in the (Gaussian chain) fit parameters relative to those used to generate the non-Gaussian properties are discussed. Only linear chains and regular stars are investigated; the results for other geometries are expected to be intermediate to these cases.

II. The Ptitsyn–Eizner Prescription

The Gaussian bead–spring model was first modified to include non-Gaussian effects (linear chains) by Ptitsyn and Eizner.[3-5] Since then their approach has been employed by Tschoegl,[6] Bloomfield and Zimm,[7] and Bloomfield and Sharp[8] to investigate low-frequency viscoelastic (VE) properties of infinitely long linear chains, rings, and regular stars. The justification for their approximate corrections

†Current address: Polymer Products Department, E. I. du Pont de Nemours and Co., Inc., PO Box 80269, Wilmington, DE 19880-0269.

0024-9297/89/2222-3435$01.50/0

was based on the results of Ptitsyn and Eizner's more rigorous model[5] which introduced non-Gaussian effects into the theory of Kirkwood and Riseman.[9] An important conclusion of the more rigorous model was that many chain properties, such as the intrinsic viscosity and the translational and rotational friction coefficients, are most sensitive to the overall dimensions of the chain. Hence to improve the predictions of the Gaussian model for properties measured in good solvents, they allowed the chain to expand relative to its Θ-solvent dimensions. Their implementation of this modification resulted in a model that has a mathematically tractable solution regardless of the choice of the (mean) expanded dimensions. When applied to predict the modified intrinsic birefringence or modified intrinsic viscoelastic properties[1] for solutions containing flexible homopolymers, the reduced magnitude of these quantities is given by

$$\frac{[\eta_{M\Delta}]}{[\eta_{M\Delta 0}]} = \frac{[S_{M\Delta}]}{[S_{M\Delta 0}]} = \left[\left(\sum_p \frac{\lambda_1/\lambda_p}{1+(\omega\tau_1)^2(\lambda_1/\lambda_p)^2}\right)^2 + \left(\omega\tau_1 \sum_p \frac{(\lambda_1/\lambda_p)^2}{1+(\omega\tau_1)^2(\lambda_1/\lambda_p)^2}\right)^2\right]^{1/2} / \sum_p (\lambda_1/\lambda_p) \quad (1)$$

while the reduced angle is

$$[\Phi_\Delta] - [\Phi_{\Delta 0}] = -([\Theta_\Delta] - [\Theta_{\Delta 0}]) = \tan^{-1}\left[\frac{\omega\tau_1 \sum_p \frac{(\lambda_1/\lambda_p)^2}{1+(\omega\tau_1)^2(\lambda_1/\lambda_p)^2}}{\sum_p \frac{\lambda_1/\lambda_p}{1+(\omega\tau_1)^2(\lambda_1/\lambda_p)^2}}\right] \quad (2)$$

Here $\sum_p$ indicates a sum over all normal modes of motion of the model, $\omega\tau_1$ is a reduced frequency, τ_1 is the longest relaxation time, λ_p is the pth positive eigenvalue of a symmetric matrix $\mathbf{L}$ of order N_s, and N_s is the number of springs in the model chain. The $\mathbf{L}$ matrix summarizes the hydrodynamic interactions between the beads representing frictional sites for the various submolecules of the chain. The general form of its elements is

$$L_{ij} = H_{i+1,j+1} + H_{ij} - H_{i+1,j} - H_{i,j+1} \quad (3)$$

where

$$H_{\nu\mu} = \delta_{\nu\mu} + (1-\delta_{\nu\mu})\left(\frac{\zeta}{6\pi\eta_e}\langle r_{\nu\mu}^{-1}\rangle\right) \quad (4)$$

ζ is the friction coefficient of each bead, $\langle r_{\nu\mu}^{-1}\rangle$ is the mean inverse distance between beads ν and μ, $\delta_{\nu\mu}$ is the Kronecker δ, and η_e is a frequency-independent environmental viscosity. Historically, η_e has been assumed to be identical with the bulk solvent viscosity η_s, or to $\phi\eta_s$ (with ϕ the volume fraction of solvent). Equations 1–4 are applicable to Gaussian or non-Gaussian chains. Non-Gaussian modifications are introduced through $\langle r_{\nu\mu}^{-1}\rangle$ in eq 4 and are the subject of the next sections.

A. Linear Chains: Uniform Expansion. The uniform expansion of Peterlin[10] assumes that $\langle r_{\nu\mu}^2\rangle$ in good solvents is described by the empirical relation $\langle r_{\nu\mu}^2\rangle = \alpha^2 b_0^2 |\nu-\mu|^{1+\epsilon}$, where α and ϵ are chain expansion parameters and b_0^2 is the mean square distance between connected beads under Θ conditions in a quiescent solution. In the original framework of Ptitsyn and Eizner, α and ϵ are assumed to be coupled and to increase from their Gaussian values ($\alpha = 1$, $\epsilon = 0$) as the chain is introduced into better solvating conditions. However, since the effects on dynamic properties due to changes in α or b_0 are indistinguishable, it is more usual to write $\langle r_{\nu\mu}^2\rangle = b^2|\nu-\mu|^{1+\epsilon}$ with b^2 representing the mean-square distance between connected beads regardless of the solvating conditions. In this way b^2 includes both long-range (α) and short-range (b_0) interactions along the chain contour. Tschoegl[6] has shown that ϵ has an upper bound of $^1/_3$ for flexible chains; Bloomfield and Zimm[7] use ϵ as large as $^1/_2$ to describe non-Gaussian effects in mechanically stiff chains.

The relationship $\langle r_{\nu\mu}^{-1}\rangle = (\langle r_{\nu\mu}^2\rangle\pi/6)^{-1/2}$ is used to approximate $\langle r_{\nu\mu}^{-1}\rangle$ from the assumed form of $\langle r_{\nu\mu}^2\rangle$; this relationship is exact only for Gaussian chains. The $\mathbf{L}$ matrix for linear chains composed of N_s springs then has the form

$$L_{ij} = a(|i-j|+1) \qquad i,j = 1, 2, 3, ..., N_s \quad (5)$$

with

$$a(i) = 2[h_\epsilon(0) - h_\epsilon(1)] \qquad i = 1$$
$$a(i) = 2h_\epsilon(i-1) - h_\epsilon(i) - h_\epsilon(i-2) \qquad i = 2, 3, 4, ..., N_s \quad (6)$$

$$h_\epsilon(n) = 1 \qquad n = 0$$
$$h_\epsilon(n) = h^*(2/n^{1+\epsilon})^{1/2} \qquad n = 1, 2, 3, ..., N_s \quad (7)$$

$$h^* = \frac{\zeta}{\eta_\epsilon}\left(\frac{1}{12\pi^3\alpha^2 b_0^2}\right)^{1/2} \quad (8)$$

when the springs are numbered consecutively along the chain contour from 1 to N_s. The dimensionless hydrodynamic interaction parameter h^* used here differs slightly from that originally proposed by Thurston and Peterlin[11] in that the $2^{\epsilon/2}$ factor is omitted to make it independent of ϵ. The so-called "free-draining" and "non-free-draining" limits of h^* are still approximately 0.00 and 0.25, respectively. (The $h^* = 0.00$ limit is not physically realistic since it implies that there is no viscous dissipation of energy ($\zeta = 0$) due to the presence of the chain. Thus whenever h^* is shown equal to 0, it denotes the limit $h^* \to 0$). Note that in this treatment the level of hydrodynamic interaction is sensitive to excluded volume effects since h^* now has an explicit dependence on α. The $\mathbf{L}$ matrix has the same basic form as that for Gaussian chains; its eigenvalues $\lambda_p(N_s,h^*,\epsilon)$ can be computed from the more concise block-diagonal forms reported elsewhere[12] simply by using the above definition of $a(i)$.

B. Regular Stars: Nonuniform Expansion. Non-Gaussian dimensions for flexible, regular star homopolymers have been obtained recently by Miyake and Freed[13,14] using the renormalization group method. Their results are valid only for small expansions of regular stars from their Θ-solvent dimensions and for chains with seven arms or less; their results for linear chains (two-armed stars) are expected to be superior to the empirical uniform expansion of Peterlin. Two forms for the mean inverse intersegmental dimensions are reported depending on whether the two Kuhn statistical segments are located on the same or different branches. Our incorporation of these results into the bead–spring model (each Gaussian submolecule containing several Kuhn statistical segments) yields

$$\langle r_{\nu\mu}^{-1}\rangle = F\left(\frac{\pi d}{Lb}\right)^{1/2}\left(\frac{2\pi N_0}{L}\right)^{-\nu_0}(x-y)^{-\nu_0}\exp\left(-\frac{\epsilon_0}{8}\frac{\zeta_0}{1+\zeta_0}[A+(f-1)B]\right) \quad (9)$$

for beads ν and μ located on the same branch ($\nu > \mu$) and

$$\langle r_{\nu\mu}^{-1} \rangle = F\left(\frac{\pi d}{Lb}\right)^{1/2}\left(\frac{2\pi N_0}{L}\right)^{-\nu_0}(x + y)^{-\nu_0} \exp\left(-\frac{\epsilon_0}{8}\frac{\zeta_0}{1+\zeta_0}[A' + (f-2)B']\right) \quad (10)$$

for beads located on different branches. For both cases d is the dimensionality of the space (set to 3 for all results reported here), $\epsilon_0 = 4 - d = 1$, f is the functionality of the regular star at the center bead, $F \simeq (\pi^{1/2}/2)[1 - (1 - 2 \ln 2)\epsilon_0/2] + \mathcal{O}(\epsilon_0^2)$ (exactly $(4/\pi)^{1/2}$ for Gaussian chains), L is the length scale in which the cooperative effects of excluded volume are summarized, b is again the root-mean-square distance between connected beads in a quiescent solution, N_0 is the contour length of a branch ($N_0 = bn_b$), n_b is the number of beads per branch, x (or y) is the fractional contour distance of bead ν (or μ) from the center bead, ν_0 is the exponent $[1 + (\epsilon_0/8)(\zeta_0/(1+\zeta_0))]/2 + \mathcal{O}(\epsilon_0^2)$, ζ_0 is the crossover parameter that indicates the degree of excluded volume effects in the chain, and, finally, the quantities A, B, A', and B' are complicated functions of x and y:

$$A = \tfrac{5}{2} + \ln\{2/[(1-x)y]\} + [2/(x-y)]\{(1-x+y)^{1/2} - (2x-y)(y/x)^{1/2} - (1+x-2y)[(1-x)/(1-y)]^{1/2}\} + 2\ln\{2(x^{1/2}+y^{1/2})[(1-x)^{1/2} + (1-y)^{1/2}]/[1+(1-x+y)^{1/2}]\} - [(x-y)/(1-x)] \times \{\Psi([(x-y)/(4-3x-y)]^{1/2}, [(x-y)/(1-y)]^{1/2}) - 1\} - [(x-y)/y]\{\Psi([(x-y)/(x+3y)]^{1/2}, [(x-y)/x]^{1/2}) - 1\} - (x-y)/(xy)^{1/2} - (x-y)/[(1-x)(1-y)]^{1/2} \quad (11)$$

$$B = \ln[2y/(1+y)] + [2/(x-y)]\{[2(2-x+y)]^{1/2} - (1-x+y)^{1/2} - (1+2x-y)[(1+y)/(1+x)]^{1/2} + (2x-y)(y/x)^{1/2}\} + 2\ln\{[1+(1-x+y)^{1/2}][(1+x)^{1/2} + (1+y)^{1/2}]/[(2^{1/2}+(2-x+y)^{1/2})(x^{1/2}+y^{1/2})]\} + [(x-y)/y] \times \{\Psi([(x-y)/(x+3y)]^{1/2}, [(x-y)/x]^{1/2}) - 1\} + (x-y) \times (xy)^{1/2} - [(x-y)/(1+y)]\{\Psi([(x-y)/(4+x+3y)]^{1/2}, [(x-y)/(1+x)]^{1/2}) - 1\} - (x-y)/[(1+x)(1+y)]^{1/2} \quad (12)$$

$$A' = \tfrac{5}{2} + \ln\{4/[(1-x)(1-y)]\} + [2/(x+y)] \times \{[2(2-x-y)]^{1/2} - (1+x+2y)[(1-x)/(1+y)]^{1/2} - (1+2x+y)[(1-y)/(1+x)]^{1/2}\} + 2\ln\{2[(1-x)^{1/2} + (1+y)^{1/2}][(1+x)^{1/2} + (1-y)^{1/2}]/[2^{1/2}+(2-x-y)^{1/2}]\} - [(x+y)/(1-x)]\{\Psi([(x+y)/(4-3x+y)]^{1/2}, [(x+y)/(1+y)]^{1/2}) - 1\} - (x+y)/[(1-x)(1+y)]^{1/2} - (x+y)/[(1+x)(1-y)]^{1/2} - [(x+y)/(1-y)] \times \{\Psi([(x+y)/(4+x-3y)]^{1/2}, [(x+y)/(1+x)]^{1/2}) - 1\} \quad (13)$$

$$B' = 2 + 2\ln[2(x+y)] - (x+y)\{\Psi([(x+y)/(4+x+y)]^{1/2}, x/[(x+y)(1+x)]^{1/2}) + \Psi([(x+y)/(4+x+y)]^{1/2}, y/[(x+y)(1+y)]^{1/2}) - 2\} - [(x+y)(x+y+xy)/(1+x)]^{1/2} - [(x+y)(x+y+xy)/(1+y)]^{1/2} + (2/x^2)\{[2(x+y)(2[x+y]-x^2)]^{1/2} - [(x+y)(x+y-x^2)]^{1/2} - (1+2x)[(x+y)(x+y+xy)/(1+x)]^{1/2}\} + (4/x)[(x+y)y]^{1/2} + (2/y^2)\{[2(x+y)(2[x+y]-y^2)]^{1/2} - [(x+y)(x+y-y^2)]^{1/2} - (1+2y)[(x+y)(x+y+xy)/(1+y)]^{1/2}\} + (4/y)[x(x+y)]^{1/2} + 2\ln\{2[(x+y)^{1/2} + (x+y-x^2)^{1/2}][((x+y)(1+x))^{1/2} + (x+y+xy)^{1/2}]/[([2(x+y)]^{1/2} + [2(x+y)-x^2]^{1/2})([x+y]^{1/2} + y^{1/2})^2]\} + 2\ln\{2[(x+y)^{1/2} + (x+y-y^2)^{1/2}][((x+y)\times(1+y))^{1/2} + (x+y+xy)^{1/2}]/[([2(x+y)]^{1/2} + [2(x+y)-y^2]^{1/2})([x+y]^{1/2} + x^{1/2})^2]\} \quad (14)$$

with

$$\Psi(k, \cos\phi) = \int_\phi^{\pi/2}(1 - k^2\sin^2\theta)^{1/2}\,d\theta/k \quad (15)$$

Here we have added subscripts to model parameters ϵ, N, ν, and ζ relative to those originally used by Miyake and Freed to avoid conflict with parameters already defined. The expression we use for F, $(4/\pi)^{1/2} \simeq 1.128$, is higher by only 7% relative to the $(\pi^{1/2}/2)[1 - (1 - 2\ln 2)\epsilon_0/2] + \mathcal{O}(\epsilon_0^2) \simeq 1.057$ arising from the renormalization group method and is used so that $b\langle r_{\nu\mu}^{-1}\rangle$ reduces to the Gaussian expression when $\zeta_0 = 0$. Of course, strictly speaking, the Gaussian limit in this model is reached when $\zeta_0 = 0$ *and* $b = b_0$, and the asymptotic self-avoiding limit of fully developed excluded volume is reached as $\zeta_0 \to \infty$. The **L** matrix for these regular stars can be divided into f symmetric submatrices (each of order n_b) along the diagonal with elements

$$U_{ij} = H_{ij} + H_{i-1,j-1} - H_{i,j-1} - H_{i-1,j} \quad (16)$$

and everywhere else symmetric submatrices of order n_b with elements

$$W_{ij} = -[H'_{ij} + H_{i-1,j-1} - H'_{i,j-1} - H'_{i-1,j}] \quad (17)$$

as found[12] for Gaussian chains. The symmetric matrix **H**, of order $n_b + 1$, summarizes the hydrodynamic interactions between beads on the same branch; its form above assumes that the beads are numbered consecutively along the contour from the center ($\nu = 0$) to the branch end ($\nu = n_b$). Its elements are

$$H_{\nu\mu} = \delta_{\nu\mu} + (1 - \delta_{\nu\mu})h^x\left(\frac{1}{2\pi}\frac{L}{b}\right)^{\nu_0}(\nu - \mu)^{-\nu_0}\exp\left(-\frac{\epsilon_0}{8}\frac{\zeta_0}{1+\zeta_0}[A + (f-1)B]\right) \quad (18)$$

when $\nu \geq \mu$. The symmetric matrix **H'**, also of order $n_b + 1$, summarizes the hydrodynamic interaction between beads on different branches, and its elements are

$$H'_{\nu\mu} = h^x\left(\frac{1}{2\pi}\frac{L}{b}\right)^{\nu_0}(\nu + \mu)^{-\nu_0}\exp\left(-\frac{\epsilon_0}{8}\frac{\zeta_0}{1+\zeta_0}[A' + (f-2)B']\right) \quad (19)$$

for any ν or μ. A, A', B, and B' are evaluated in terms of $x = \nu/n_b$ (or $y = \mu/n_b$), and a new dimensionless hydrodynamic interaction parameter h^x given by

$$h^x = \frac{\zeta}{\eta_e}\left(\frac{1}{3\pi^2 Lb}\right)^{1/2} \quad (20)$$

which varies between 0 and $(\pi b/4L)^{1/2}$. These limits on h^x are the free-draining and non-free-draining limits, respectively. The upper limit is found from the correspondence of this model when $\zeta_0 = 0$ to that of the Gaussian model at the non-free-draining limit ($h^* = 0.25$)

and is assumed to be applicable for any ζ_0. For example, comparison of eq 18 (or eq 19) when $\zeta_0 = 0$ with those for Gaussian chains yields the correspondence

$$h^* = \left(\frac{L/b}{4\pi}\right)^{1/2} h^x \qquad (21)$$

and the upper limit for h^x is obtained when $h^* = 0.25$. L is a phenomenological length scale[13,14] assumed to vary between b and $n_b b$, so h^x is not expected to exceed $(\pi/4)^{1/2} \simeq 0.89$. Note again that the level of hydrodynamic interaction is sensitive to excluded volume effects since h^x depends on Lb. The eigenvalues $\lambda_p(n_b,f,h^x,L/b,\zeta_0)$ of $\mathbf{L}$ can be computed from the same block-diagonal form reported elsewhere[12] for Gaussian chains simply by using these new definitions for submatrices $\mathbf{U}$ and $\mathbf{W}$.

III. Computation of Eigenvalues

Fortran software,[1] which enables all N_s eigenvalues to be computed exactly for Gaussian chains, was modified to compute those for non-Gaussian chains. Only the matrix generation section required modification, as detailed in section II, since the numerical eigenvalue routine is applicable to any real symmetric matrix. The reliability of the software to generate these new matrices is indicated by its ability to recover Gaussian properties (when $\epsilon = 0$, or when $\zeta_0 = 0$), and its ability to reproduce the mean inverse interbead dimensions reported in Figures 3 and 4 of ref 13. The latter is a nontrivial problem that requires removal of the many singularities in eq 11–14 when x (or y) approaches 0 or 1; use of the approximation

$$\Psi(1 - \lambda_0, 1 - \mu_0) = 1 + (\lambda_0/2)(3 \ln 2 + 1 + \ln \lambda_0) - (2\mu_0)^{1/2} + \ldots \qquad (22)$$

which is valid for $\lambda_0 > 0$ and $\mu_0 \ll 1$, simplifies this endeavor.

The computations were done in double precision (Harris/7, VAX 8800) or single precision (Cray X-MP/24). The Cray was used on the longer chains to substantially reduce the required CPU time. For example, the time required to obtain the properties of a regular star (n_b = 500) with the Miyake–Freed interbead dimensions dropped from 6 h to 5 min. The absolute eigenvalue accuracy was evaluated as before[1] and found to be $\pm 10^{-7}$ for each eigenvalue. This guarantees the relative accuracy of the smaller eigenvalues—important because they dominate the low-frequency properties—to three or more significant figures. The matrices and eigenvalues for a small linear chain and a regular star are found in the Appendix.

IV. Excluded Volume Effects in Linear Chains

The property of interest is the frequency dependence of $[S^*]_\Delta/[S_0]_\Delta$ (or $[\eta^*]_\Delta/[\eta_0]_\Delta$) as expressed by eq 1 and 2. This dependence, especially that of the reduced angle, has excellent potential for characterization of the long-chain structure for homopolymers when it can be measured over the range of frequencies $0.1/\tau_1 < \omega < 10/\tau_N$. The effects of excluded volume on this dependence, in the approximate framework of Ptitsyn and Eizner, can now be investigated by choosing values of h^* and ϵ for linear chains, or h^x, L/b, and ζ_0 for regular stars. At this point, choosing values that would always realistically fit measured properties is difficult because each set of excluded volume parameters is intimately coupled in a manner that is poorly understood. Recognizing this, in the subsections that follow, each parameter is treated at first as an independent variable.

A. Uniform Expansion. The effect of uniform expansion on the frequency dependence of $[S^*]_\Delta/[S_0]_\Delta$ and on the relaxation time spectrum for the model chain is

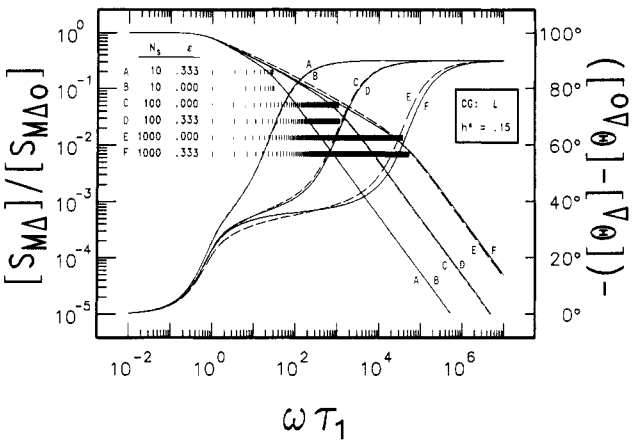

Figure 1. Predicted effects of uniform expansion parameter ϵ on dynamic properties of linear chains for the Ptitsyn–Eizner model when $h^* = 0.15$; Gaussian limit ($\epsilon = 0$) shown with broken lines.

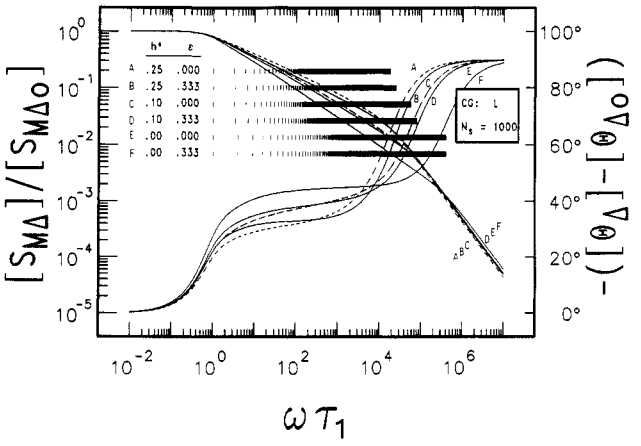

Figure 2. Predicted effects of uniform expansion parameter ϵ on dynamic properties of linear chains for the Ptitsyn–Eizner model when $N_s = 1000$; Gaussian limit ($\epsilon = 0$) shown with broken lines.

shown in Figures 1 and 2. In these figures, as well as those that follow, the logarithm of the reduced magnitude $\log_{10}([S_{M\Delta}]/[S_{M\Delta 0}])$ and the reduced angle $-([\Theta_\Delta] - [\Theta_{\Delta 0}])$ are both plotted as ordinates against the logarithm of the reduced angular shearing frequency $\log_{10}(\omega\tau_1)$. The relaxation time spectrum is drawn as a set of vertical lines along the reduced frequency axis; each line represents a normal mode of motion of the bead–spring chain and the pth mode line is plotted where $\omega = 1/\tau_p$. When degeneracies occur, as in the case of regular stars, the individual lines are drawn so that the height of the line is proportional to the degeneracy. The properties of several chains are always displayed on a single plot. The model parameters under study are listed to the left of each relaxation time spectrum; those parameters held fixed are shown in the box on the right side of the figure. The chain geometry, either linear or regular star, is indicated with uppercase letters—L or S—under the heading CG. The predictions of the dynamic properties for chains that have $b\langle r_{\nu\mu}^{-1}\rangle = [6/(\pi|\nu - \mu|)]^{1/2}$ (the result for Gaussian chains) are always drawn with broken lines to make them distinct. These chains with $\epsilon = 0$, or later with $\zeta_0 = 0$, have b expanded relative to its size b_0 in a Θ solvent and are of interest because their properties are indistinguishable from those of Gaussian chains when computed for the same N_s and h^*. Hence in the subsequent discussions we will loosely label such expanded chains as Gaussian and interpret h^* in the Ptitsyn–Eizner framework as a hydrodynamic in-

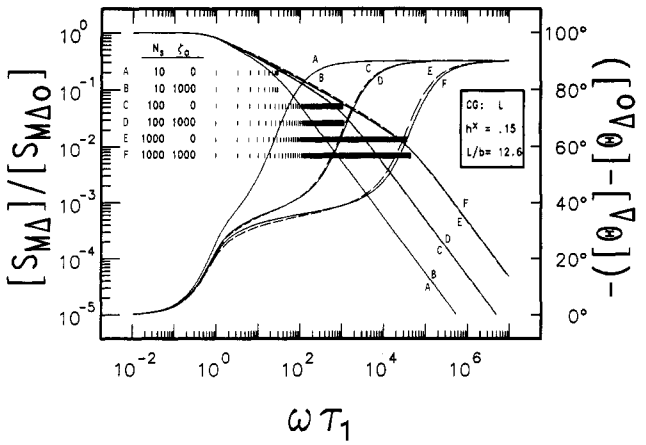

Figure 3. Predicted effects of nonuniform expansion parameter ζ_0 on dynamic properties of linear chains for the Ptitsyn–Eizner model when $h^x = 0.15$ and $L/b = 12.6$; Gaussian limit ($\zeta_0 = 0$) shown with broken lines.

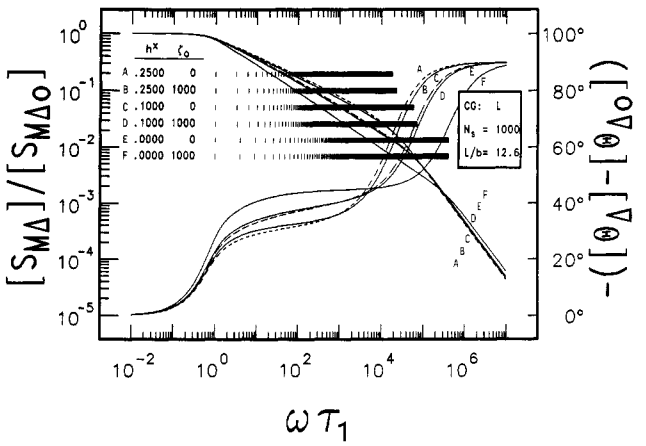

Figure 4. Predicted effects of nonuniform expansion parameter ζ_0 on dynamic properties of linear chains for the Ptitsyn–Eizner model when $N_s = 1000$ and $L/b = 12.6$; Gaussian limit ($\zeta_0 = 0$) shown with broken lines.

teraction parameter sensitive to excluded volume effects.

The predictions shown in Figure 1 are for Gaussian chains ($\epsilon = 0$) and non-Gaussian chains ($\epsilon = 0.333$) for selected N_s at $h^* = 0.15$. The ϵ chosen for the non-Gaussian chains is the maximum value expected for flexible homopolymers, so typical effects of ϵ on the reduced dynamic properties are expected to be intermediate to these extremes. The maximum effect of ϵ is small for chains composed of about 100 springs or less. The differences are so small that the two (solid and broken-line) curves for $N_s = 10$ and the two for $N_s = 100$, appear in the figure as nearly indistinguishable lines. Thus reliable estimates of ϵ arising from fitting such non-Gaussian predictions to measured properties of chains with molecular weights of 2×10^5 or less are expected to be difficult. However, at larger N_s, the effect of ϵ is more pronounced, and it may be possible to use ϵ as a fit parameter. Three effects are observed as ϵ increases from 0 to 0.333: the spacings between adjacent relaxation times widen, the low-frequency portion of the plateau in the reduced angle rises, and the entire plateau in the reduced angle widens. All three effects are very similar to those observed when h^* decreases as discussed in more detail in section IV.C; this contributes to the difficulty of differentiating between the effects of hydrodynamic interaction and excluded volume already inherent in the definition of h^*.

The effects of h^* and ϵ are contrasted for $N_s = 1000$ in Figure 2 (corresponds to a molecular weight greater than 10^6). A large value of N_s was chosen to enhance the effect of ϵ. The effect of ϵ on the dynamic properties is small relative to h^*; it has no effect at the free-draining limit, $h^* \to 0$, but becomes more pronounced as h^* increases. The largest effect is seen at the non-free-draining limit ($h^* \simeq 0.25$), but this result is misleading because of our arbitrary choice to adjust h^* and ϵ as independent parameters in this section. More realistically, it is expected that as the non-free-draining limit is approached, Gaussian statistics would be recovered (approximately) so that ϵ would tend to vanish rather than remain at 0.333 as used in the figure.

B. Nonuniform Expansion. Predictions of excluded volume effects for linear chains in which nonuniform expansion is occurring are shown in Figures 3 and 4. They arise from specializing predictions for regular stars to two-armed stars ($f = 2$) for which $N_s = 2n_b$. The properties of the Gaussian chains ($\zeta_0 = 0$) in Figure 3 (or Figure 4) are identical with those in Figure 1 (or Figure 2) since we have chosen $h^x = h^*$ and, as prescribed by eq 21, $L/b = 4\pi \simeq 12.6$. The choice of $\zeta_0 = 1000$ for the non-Gaussian chains is found to be a good approximation to the asymptotic self-avoiding limit ($\zeta_0 = \infty$) of fully developed excluded volume since a larger ζ_0 has no effect on the first three significant figures of the computed properties; this result undoubtedly arises because ζ_0 always appears in the computations in terms of the product $\zeta_0 (1 + \zeta_0)^{-1}$. Thus typical effects due to ζ_0 are expected to be intermediate to the illustrated extremes.

The results displayed in Figures 1 and 3 or in Figures 2 and 4 indicate that the effects of ζ_0 and ϵ are very similar with respect to the dynamic properties of Gaussian chains. Both parameters have only a small effect, and increasing either parameter widens the spacings between adjacent relaxation times, raises the low-frequency portion of the plateau in the reduced phase, and widens the breadth of the whole plateau; these effects become more pronounced as the chain size increases or as the degree of hydrodynamic interaction increases. The last result, however, is misleading as h^x or h^* approaches the non-free-draining limit; it arises only because of our unrealistic choice to vary h^x (or h^*) independent of ζ_0 (or ϵ). Excluded volume effects are also influenced by the choice of L/b. This parameter only seems to attenuate the magnitude of the effects already described in the reduced magnitude and angle. The effects are largest when $L/b = 1$ and appear to be of the same magnitude as those computed with the Peterlin expansion for $\epsilon = 0.333$. As L/b rises to $n_b/2$ (or equivalently $N_s/4$), the effect of excluded volume becomes too small to observe regardless of the value of N_s or ζ_0. We conclude from the close similarity of the effects of ζ_0 and ϵ that further refinements in $b\langle r_{\nu\mu}^{-1}\rangle$ are unnecessary for predicting dynamic OFB or VE properties of linear chains, at least within the Ptitsyn–Eizner formalism. We also note that the Miyake–Freed dimensions appear to be applicable to *linear* chains with more than just modest expansions from their Θ dimensions as the authors originally stated; otherwise the predictions of excluded volume effects on dynamic properties found here using fully expanded Miyake–Freed dimensions would not be of the same order of magnitude as a fully expanded chain with Peterlin dimensions.

C. Fitting Non-Gaussian Properties To Obtain N_s. When reduced dynamic properties (such as the frequency dependence of $[S^*]_\Delta/[S_0]_\Delta$ or $[\eta^*]_\Delta/[\eta_0]_\Delta$) measured in a good solvent are used to characterize the long-chain structure of linear chains, obtaining a reliable N_s from fits of theoretical predictions to data is more important than

obtaining parameters h^* and ϵ, or h^x, L/b, and ζ_0. Fortunately, these properties have a much stronger dependence on N_s than any other parameter; thus the prospect of achieving this objective is excellent. From Figures 1–4, non-Gaussian effects on the properties due to ϵ or ζ_0 are expected to be so small that they can be neglected for the purposes of assigning N_s. For chains with $N_s < 100$, neglect of ϵ or ζ_0 (by setting them to zero) when attempting to fit measured properties of non-Gaussian chains will have no effect on parameters N_s or h^*. For longer chains, the h^* obtained when fitting non-Gaussian properties will be slightly smaller relative to those obtained when parameters ϵ or ζ_0 are not neglected. For example, the properties predicted for a non-Gaussian chain with $N_s = 1000$, $h^* = 0.15$, and $\epsilon = 0.333$ or for one with $N_s = 1000$, $h^x = 0.15 \times (4\pi)^{1/2} \simeq 0.5317$, $L/b = 1$, and $\zeta_0 = 1000$ are both well approximated by those of a chain with $N_s = 1000$, $h^* = 0.10$, and $\epsilon = 0$; use of $h^* = 0.10$ rather than 0.15 slightly improves the mismatch in the level and the breadth of the plateau in the reduced angle. The properties predicted for the chain with $N_s = 1000$, $h^* = 0.10$, and $\epsilon = 0$ are, of course, indistinguishable from those of a Gaussian chain with $N_s = 1000$ and $h^* = 0.10$. Hence reliable values of N_s are expected when the Gaussian bead–spring model is used to fit the dynamic properties of linear homopolymers measured in a good solvent, and the value of h^* obtained from such fits should be interpreted in the Ptitsyn–Eizner framework as a hydrodynamic interaction parameter sensitive to excluded volume effects.

There is a substantial body of experimental data supporting many of these predictions for linear chains. For example, it is well-known[2] that the frequency dependence of reduced dynamic mechanical and optical properties of homopolymers dissolved in good solvents are quantitatively fit by predictions of the Gaussian bead–spring model. The empirical relation[15] $\alpha_\eta h^* = 0.21$, with expansion factor $\alpha_\eta^3 = [\eta]/[\eta]_\Theta$, found for polystyrene, poly(α-methylstyrene), and 1,4-polybutadiene (55% trans) dissolved in several solvents indicates that h^* is sensitive to excluded volume effects. The hydrodynamic interaction parameter h^* has also been reported[16–18] to decrease slightly with increasing molecular weight (N_s) when properties measured in a good solvent are fitted with Gaussian model predictions. Only the difficulty of obtaining dynamic data over a sufficiently wide range of shearing frequencies to ascertain a reliable value of fit parameter N_s in solvents at or near Θ conditions has precluded confirming that N_s is independent of the solvent. Another[19] theoretical argument suggesting that h^* is sensitive to excluded volume effects has also been proposed recently.

D. Weak Dependence of $\alpha_\eta h^*$ on Solvent Power. The origin of the empirical relation $\alpha_\eta h^* = 0.21 \pm 0.02$ reported by Osaki and co-workers[15] for linear homopolymers in solution is investigated within the Ptitsyn–Eizner treatment of excluded volume. Recall that the expansion factor $\alpha_\eta^3 = [\eta]/[\eta]_\Theta$ is obtained from intrinsic viscosity measurements, and h^* is obtained from fitting dynamic data (measured over at least 2 decades of shearing frequencies and extrapolated to infinite dilution) with the Gaussian bead–spring model. As presented in the previous sections, dynamic properties predicted with the Gaussian model are equivalent to those of the Ptitsyn–Eizner model computed at the same N_s and h^* when $\epsilon = 0$ (or $\zeta_0 = 0$) and will closely approximate non-Gaussian properties for any ϵ if an appropriate value of h^* is employed. In any solvent the intrinsic viscosity is expressed as[2]

$$[\eta] = \frac{RT}{M\eta_e}\tau_1 S_1 \tag{23}$$

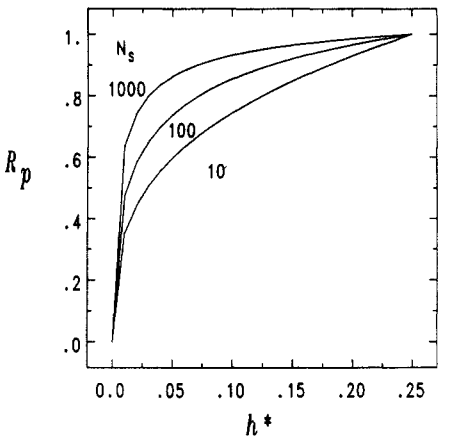

Figure 5. Dependence of R_p on h^* for linear chains composed of 10, 100, or 1000 springs as computed with the Ptitsyn–Eizner model with $\epsilon = 0$ (or $\zeta_0 = 0$) or with the Gaussian model. Θ conditions are assumed when $h^* = 0.25$.

and h^* is a hydrodynamic interaction parameter sensitive to excluded volume effects.

The longest relaxation time τ_1 is given by

$$\tau_1 = \frac{b^2\zeta}{6kT\lambda_1} \tag{24}$$

and the sum of all N_s relaxation times of the model chain normalized to τ_1 is given by $S_1 = \sum_p \tau_p/\tau_1$. Recognizing that $[\eta]$, ζ, η_e, λ_p, and h^* all depend on the solvent and subscripting each quantity with a Θ when denoting Θ conditions, one finds that

$$\alpha_\eta = \alpha R_p \tag{25}$$

with

$$R_p = \left(\frac{h^*}{h^*_\Theta}\frac{\lambda_{1,\Theta}}{\lambda_1}\frac{S_1}{S_{1,\Theta}}\right)^{1/3} \tag{26}$$

R_p monotonically increases from 0 to 1 as h^* rises from its free-draining to non-free-draining limits. This dependence is shown in Figure 5 for chains composed of 10, 100, or 1000 springs assuming $h^*_\Theta = 0.25$. R_p rises steeply to about 0.85 as h^* approaches 0.1, whereas for larger h^* it has a much weaker dependence on h^*. The data[15] used to obtain the $\alpha_\eta h^*$ relationship were always fit to Gaussian bead–spring model predictions with $h^* \geq 0.1$, so for these cases R_p can be considered to be effectively constant and close to unity. Combining eq 8, 25, and 26 yields

$$\alpha_\eta h^* = \alpha R_p h^* = R_p \frac{\zeta}{\eta_e}\left(\frac{1}{12\pi^3 b_0^2}\right)^{1/2} \tag{27}$$

a relationship that predicts $\alpha_\eta h^* = 0.25$ for Θ conditions but does not explicitly predict that $\alpha_\eta h^*$ should be independent of solvent power since the dependence of ζ/η_e on solvent power is not known. Alternatively, since $\alpha_\eta h^*$ has been observed to be approximately independent of solvent power, eq 27 predicts that ζ/η_e should be a constant. The fact that $\alpha_\eta h^*$ averaged for several polymer/solvent systems is observed to be approximately 16% smaller than 0.25 could arise from two sources. First, noting that data measured near Θ conditions often have $\alpha_\eta h^*$ exceeding 0.21 indicates that the modest change in R_p with h^* for $h^* \geq 0.1$ (can be as much as 15%) probably is contributing to this result. Another possible source of error arises from the use of the Gaussian model to assign h^*. The derivation

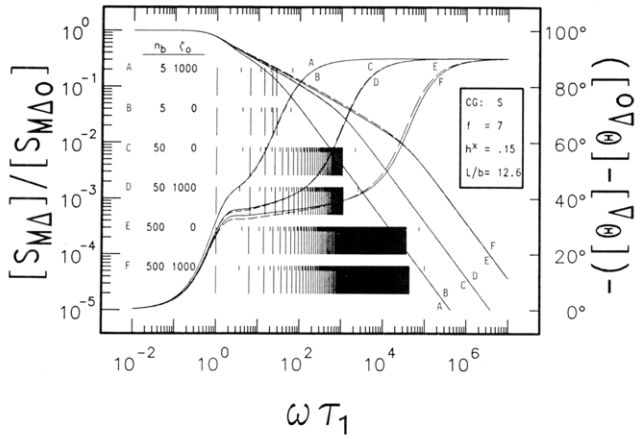

Figure 6. Predicted effects of nonuniform expansion parameter ζ_0 on dynamic properties of regular stars for the Ptitsyn–Eizner model when $h^x = 0.15$ and $L/b = 12.6$; Gaussian limit ($\zeta_0 = 0$) shown with broken lines.

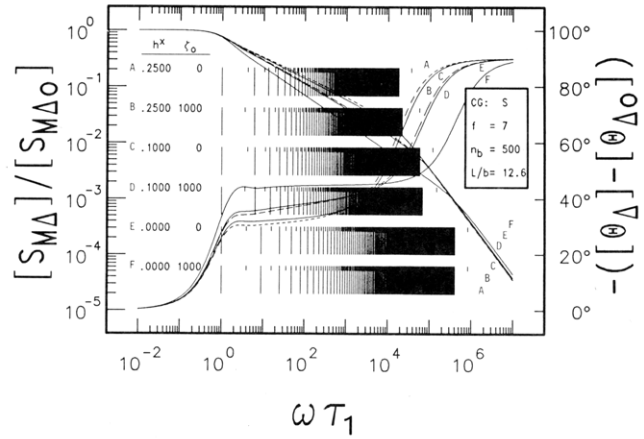

Figure 7. Predicted effects of nonuniform expansion parameter ζ_0 on dynamic properties of regular stars for the Ptitsyn–Eizner model when $n_b = 500$ and $L/b = 12.6$; Gaussian limit ($\zeta_0 = 0$) shown with broken lines.

of eq 27 assumes that h^* is obtained by fitting the dynamic data to the Ptitsyn–Eizner model using the correct ϵ. Computations reported in section IV.C indicate that the value of h^* obtained by fitting non-Gaussian properties with the Gaussian model is slightly smaller than the true value, and this systematic difference becomes more pronounced as the chain size increases and as h^* approaches 0.1. Thus it is expected that the data for the highest molecular weight sample measured in the best solvent will have the lowest $\alpha_\eta h^*$—and it does.

V. Excluded Volume Effects in Regular Stars

Non-Gaussian effects on the interbead dimensions $b\langle r_{\nu\mu}^{-1}\rangle$ are expected[13,14] to increase strongly as the number of arms, f, attached to the central bead rises. These effects are largest near the star center, and since this region of the star contributes most to $[S^*]_\Delta/[S_0]_\Delta$,[20] one would expect non-Gaussian effects to become more evident as f increases. At large f, the effects seen in regular stars should form an upper bound to the effects expected for other chain geometries (H, comb, ring, cyclic comb) with lower segmental densities. Our use of Miyake–Freed interbead dimensions, which consider only binary interactions between segments, precludes investigation of the large f limit; it is valid only for stars with $f < 8$, so the properties reported here are considered to be an upper bound only for chains with no more than 7 branches attached to any branch site. This is of minor importance for use of VE or OFB properties to characterize long-chain structure in regular stars since these properties are insensitive to f for $f > 8$.

A. Nonuniform Expansion. The effects of n_b and ζ_0 on the frequency dependence of $[S^*]_\Delta/[S_0]_\Delta$ and the relaxation time spectrum of seven-armed regular stars for $h^x = 0.15$ and $L/b = 12.6$ are illustrated in Figure 6. Again the two values of ζ_0 chosen for this figure represent the Gaussian limit and the asymptotic self-avoiding limit of fully developed excluded volume, so typical effects due to ζ_0 should be intermediate to those illustrated here. The effects of ζ_0 on the reduced magnitude and angle are so small for $n_b = 5$ (or 50) that the solid and broken-line curves—corresponding to ζ_0 of 1000 and 0, respectively—almost appear to be a single line. The effects of ζ_0 become more pronounced as n_b rises, and when n_b exceeds 100 it may be necessary to fit such dynamic properties with ζ_0. These effects are very similar to those found for linear chains; see section IV.B and Figure 3. The properties displayed in Figures 3 and 6 are computed for the same n_b, h^x, L/b, and ζ_0 to facilitate a comparison between both geometries. The only difference observed is that the spacing between the first degenerate and first nondegenerate relaxation time decreases in these stars as ζ_0 rises.

The effects of h^x and ζ_0 are contrasted in Figure 7 for seven-armed regular stars with $n_b = 500$ (arm molecular weight of approximately 5×10^5 or greater) and $L/b = 12.6$. The large n_b is chosen to enhance the effects due to ζ_0. The effects of ζ_0 are small relative to those of h^x but become more pronounced as h^x increases. The largest effect appears to be at the non-free-draining limit ($h^x = 0.25$), but this result is again an artifact of varying ζ_0 and h^x independently. Note also that the effects due to f are modest. This can be seen by comparing the predictions for $f = 2$ in Figure 4 to those of $f = 7$ in Figure 7; both sets were computed for the same h^x and L/b.

B. Fitting Non-Gaussian Properties To Obtain n_b and f. As for linear chains, the frequency dependence of the reduced magnitude or angle of $[S^*]_\Delta/[S_0]_\Delta$ or $[\eta^*]_\Delta/[\eta_0]_\Delta$ are not strongly dependent on ζ_0, and properties for $\zeta_0 > 0$ are well approximated by setting $\zeta_0 = 0$ and using a slightly smaller h^x. We recommend, when $f < 8$ and reliable estimates of only n_b and f are desired, that the properties of regular stars measured under non-Θ conditions simply be fitted to predictions of the non-Gaussian model (n_b, f, h^x, L/b, ζ_0) with $\zeta_0 = 0$, or equivalently with predictions of the Gaussian model (n_b, f, and h^*) and interpret h^* as a hydrodynamic interaction parameter sensitive to excluded volume effects. Comparisons between dynamic properties of regular stars measured under non-Θ conditions and those predicted by the Gaussian model will be reported soon.[21]

VI. Conclusions

Gaussian bead–spring model predictions are expected to provide very good fits to the frequency dependence of modified intrinsic birefringence $[S^*]_\Delta$ and the modified complex viscosity $[\eta^*]_\Delta$ coefficients for solutions containing flexible homopolymers when measured in good solvents. The model parameters arising from fits of these properties should still quantitatively reflect the long-chain structure of the homopolymer. The hydrodynamic interaction parameter h^* required for such fits is expected to be sensitive to excluded volume effects. This sensitivity arises from the explicit dependence of h^* on the interbead expansion parameter α (eq 8) and implicitly from the neglect of the Gaussian model to use more realistic mean inverse interbead dimensions $b\langle r_{\nu\mu}^{-1}\rangle$. The latter effect is expected to cause the h^* deduced from fits of Gaussian predictions to data measured in good solvents to be slightly smaller than

that deduced with the non-Gaussian model of Ptitsyn and Eizner using the correct ϵ. The systematic error becomes more pronounced as the chain size increases and is expected to be observable for linear homopolymers modeled with chains composed of about 200 springs or more (molecular weights exceeding about 3×10^5). It is this effect in linear chains that may be responsible for the small decreases in h^* required to fit dynamic data with the Gaussian model as the homopolymer molecular weight rises. Use of the Gaussian model to interpret long-chain structure from dynamic data measured in good solvents based on computations advanced here should be limited to chains with less than eight arms attached to any branch site. For regular stars this is not a serious limitation since the properties become independent of f for $f > 8$. These results extend our previous Θ-solvent predictions[1] of the excellent ability of dilute-solution dynamic experiments to characterize long-chain structure in flexible homopolymers to properties measured in any solvent.

Caution is advised when extending these results to solution dynamics experiments other than linear viscoelasticity and oscillatory flow birefringence. Other experiments, such as scattering studies, are more sensitive to the non-Gaussian nature of homopolymers in good solvents.

Acknowledgment. We express our appreciation to Dr. J. F. Douglas, Professors K. F. Freed and A. Miyake, and Emeritus Professor J. D. Ferry for helpful discussions. This work was supported by the National Science Foundation Polymers Program through Grant Nos. DMR-7925020, DMR-8303207, and DMR-8800641.

Appendix

The matrices and eigenvalues of a small linear chain and a regular star are reported for those interested in duplicating or extending these numerical computations. These results will be particularly helpful for those interested in the Miyake–Freed computations since the limiting expressions for eq 11–14 when x (or y) approaches 0 or 1 are not in print.

The dynamic properties of a linear chain ($N_s = 8$, $h^* = 0.15$, $\epsilon = 0.333$) when employing the uniform expansion of Peterlin are computed by diagonalizing two symmetric submatrices each of order $N_s/2$. The first submatrix, $\mathbf{L}^o$, contains the odd-indexed eigenvalues:

$$\mathbf{L}^o = \begin{bmatrix} 0.866\,350 & -0.756\,219 & -0.060\,685 & -0.020\,013 \\ & 1.561\,884 & -0.715\,547 & -0.050\,166 \\ & & 1.572\,403 & -0.711\,415 \\ & & & 1.574\,399 \end{bmatrix} \quad \text{(A.1)}$$

Its eigenvalues are 0.144 409, 0.917 283, 1.877 859, and 2.635 485 after rounding to $\pm 10^{-6}$. The second submatrix, $\mathbf{L}^e$, contains the even-indexed eigenvalues:

$$\mathbf{L}^e = \begin{bmatrix} 2.285\,122 & -0.662\,554 & -0.032\,981 & -0.007\,692 \\ & 1.589\,588 & -0.703\,226 & -0.043\,500 \\ & & 1.579\,069 & -0.707\,357 \\ & & & 1.577\,073 \end{bmatrix} \quad \text{(A.2)}$$

Its eigenvalues are 0.479 905, 1.400 879, 2.302 440, and 2.847 627.

The dynamic properties of a regular star ($n_b = 4$, $f = 3$, $h^x = 0.376$, $L/b = 2$, $\zeta_0 = 1000$) when employing the nonuniform expansion of Miyake and Freed are computed by diagonalizing two symmetric submatrices each of order n_b. The first submatrix, $\mathbf{L}^o = \mathbf{U} - \mathbf{W}$, contains the odd-indexed eigenvalues:

$$\mathbf{L}^o = \begin{bmatrix} 0.885\,762 & -0.802\,992 & -0.042\,512 & -0.012\,762 \\ & 1.639\,870 & -0.771\,246 & -0.031\,525 \\ & & 1.640\,989 & -0.759\,862 \\ & & & 1.614\,357 \end{bmatrix} \quad \text{(A.3)}$$

Its eigenvalues are 0.138 478, 0.910 181, 1.937 409, and 2.794 910. The second submatrix, $\mathbf{L}^e = \mathbf{U} + (f - 1)\mathbf{W}$, contains the even-indexed eigenvalues:

$$\mathbf{L}^e = \begin{bmatrix} 3.251\,908 & -0.718\,656 & -0.017\,827 & -0.004\,761 \\ & 1.667\,300 & -0.759\,420 & -0.026\,744 \\ & & 1.647\,052 & -0.757\,296 \\ & & & 1.615\,031 \end{bmatrix} \quad \text{(A.4)}$$

Its eigenvalues are 0.502 814, 1.523 594, 2.579 484, and 3.575 399.

References and Notes

(1) Sammler, R. L.; Schrag, J. L. *Macromolecules* **1988**, *21*, 3273.
(2) Ferry, J. D. *Viscoelastic Properties of Polymers*, 3rd ed.; Wiley: New York, 1980.
(3) Ptitsyn, O. B. *Zh. Fiz. Khim.* **1957**, *31*, 1091.
(4) Ptitsyn, O. B.; Eizner, Yu. E. *Zh. Fiz. Khim.* **1958**, *32*, 2464.
(5) Ptitsyn, O. B.; Eizner, Yu. E. *Zh. Tekh. Fiz.* **1959**, *29*, 1117.
(6) Tschoegl, N. W. *J. Chem. Phys.* **1964**, *40*, 473.
(7) Bloomfield, V. A.; Zimm, B. H. *J. Chem. Phys.* **1966**, *44*, 315.
(8) Bloomfield, V. A.; Sharp, P. A. *Macromolecules* **1968**, *1*, 380.
(9) Kirkwood, J. G.; Riseman, J. *J. Chem. Phys.* **1948**, *16*, 565.
(10) Peterlin, A. *J. Chem. Phys.* **1955**, *23*, 2464.
(11) Thurston, G. B.; Peterlin, A. *J. Chem. Phys.* **1967**, *46*, 4881.
(12) Sammler, R. L.; Schrag, J. L. *Macromolecules* **1988**, *21*, 1132.
(13) Miyake, A.; Freed, K. F. *Macromolecules* **1983**, *16*, 1228.
(14) Miyake, A.; Freed, K. F. *Macromolecules* **1984**, *17*, 678.
(15) Osaki, K.; Schrag, J. L.; Ferry, J. D. *Macromolecules* **1972**, *5*, 144.
(16) Thurston, G. B. *J. Chem. Phys.* **1967**, *47*, 3582.
(17) Sammler, R. L. Ph.D. Thesis, University of Wisconsin at Madison, 1985.
(18) Sammler, R. L.; Landry, C. J. T.; Woltman, G. R.; Schrag, J. *Macromolecules*, submitted for publication.
(19) Douglas, J. F.; Freed, K. F. *Macromolecules* **1985**, *18*, 2445.
(20) Man, V. Ph.D. Thesis, University of Wisconsin at Madison, 1984.
(21) Peterson, P. S.; Dibbs, M. G.; Sammler, R. L.; Fetters, L. J.; Roovers, J. E. L.; Schrag, J. L., manuscript in preparation.